

## Sine-Gordon field theory for the Kosterlitz-Thouless transitions on fluctuating membranes

Jeong-Man Park and T. C. Lubensky

*Department of Physics, University of Pennsylvania, Philadelphia, Pennsylvania 19104*

(Received 6 July 1995)

In the preceding paper [J. M. Park and T. C. Lubensky, *Phys. Rev. E* **53**, 2648 (1996)] we derived Coulomb-gas and sine-Gordon Hamiltonians to describe the Kosterlitz-Thouless transition on a fluctuating surface. These Hamiltonians contain couplings to a Gaussian curvature that are not found in a rigid flat surface. In this paper, we derive renormalization-group recursion relations for the sine-Gordon model using field-theoretic techniques developed to study flat space problems.

PACS number(s): 05.70.Jk, 68.10.-m, 87.22.Bt

### I. THE SINE-GORDON HAMILTONIAN

The Hamiltonian and associated partition function describing  $p$ -atic order on a fluctuating surface were derived and analyzed in the Coulomb-gas model in the previous paper [1]. The renormalization-group (RG) recursion relations for  $K$ ,  $\kappa$ , and  $y$  were also derived from the Coulomb-gas model. In addition, we described there how the two-dimensional Coulomb-gas model can be transformed into a sine-Gordon field theory.

Here we describe to what extent these results can be verified by a well-controlled renormalization procedure based on the sine-Gordon field theory. The two-dimensional Coulomb-gas model can be converted into the sine-Gordon Hamiltonian via a Hubbard-Stratonovich transformation. The advantage of this transformation is that it makes available to us standard field theory diagrammatics and renormalization procedures [2,3]. This opens up a systematic way of obtaining results for the RG recursion relations.

The  $p$ -atic membrane partition function in the sine-Gordon field theory is written as

$$\mathcal{Z} = \int \mathcal{D}\phi \mathbf{D}\mathbf{R} e^{-\beta\mathcal{H}_\kappa - \beta\mathcal{H}_\sigma - i(p/2\pi) \int d^2u \sqrt{g} S\phi}, \quad (1.1)$$

where  $\beta$  is the inverse temperature,

$$\beta\mathcal{H}_\kappa = \frac{1}{2}\beta\kappa \int d^2u \sqrt{g} H^2, \quad (1.2)$$

and

$$\beta\mathcal{H}_\sigma = \frac{1}{2\beta K} \left(\frac{p}{2\pi}\right)^2 \int d^2u \sqrt{g} g^{\alpha\beta} \partial_\alpha \phi \partial_\beta \phi - \frac{2y}{a^2} \int d^2u \sqrt{g} \cos \phi \quad (1.3)$$

with  $\frac{1}{2}H = \frac{1}{2}K_\alpha^\alpha$  the mean curvature and  $S = \det K_\beta^\alpha$  the Gaussian curvature. In the Monge gauge, the metric tensor  $g_{\alpha\beta}$  is written as

$$g_{\alpha\beta} = \partial_\alpha \mathbf{R} \cdot \partial_\beta \mathbf{R} = \begin{pmatrix} 1 + (\partial_x h)^2 & \partial_x h \partial_y h \\ \partial_x h \partial_y h & 1 + (\partial_y h)^2 \end{pmatrix}, \quad (1.4)$$

and the curvature tensor  $K_{\alpha\beta}$  is

$$K_{\alpha\beta} = \mathbf{N} \cdot D_\alpha D_\beta \mathbf{R} = \frac{1}{\sqrt{1 + (\nabla h)^2}} \begin{pmatrix} \partial_x \partial_x h & \partial_x \partial_y h \\ \partial_y \partial_x h & \partial_y \partial_y h \end{pmatrix}, \quad (1.5)$$

where  $(\nabla h)^2 = (\partial_x h)^2 + (\partial_y h)^2$ . To lowest order in  $h$ ,

$$H = g^{\alpha\beta} K_{\alpha\beta} = \partial_x \partial_x h + \partial_y \partial_y h = \nabla^2 h, \quad (1.6)$$

and

$$S = \det g^{\alpha\beta} K_{\alpha\beta} = \frac{1}{2}(\nabla^2 h \nabla^2 h - \partial_i \partial_j h \partial_i \partial_j h). \quad (1.7)$$

In performing a perturbation calculation with Hamiltonian (1.2) and (1.3) in two dimensions, one faces infrared as well as ultraviolet divergences. For the infrared regularization, we introduce a tension term,

$$\beta\mathcal{H}_\sigma = \beta\sigma \int d^2u \sqrt{g} \cong \beta\sigma \int d^2x [1 + \frac{1}{2}(\nabla h)^2] \quad (1.8)$$

into the bending Hamiltonian (1.2) and a mass term

$$\beta\mathcal{H}_m = \frac{1}{2\beta K} \left(\frac{p}{2\pi}\right)^2 \int d^2u \sqrt{g} m^2 \phi^2 \quad (1.9)$$

into the sine-Gordon Hamiltonian (1.3). Our infrared treatment is similar to the infrared regularization in Ref. [3]. After perturbation theory is summed, we shall see that our renormalization-group recursion relations have a well-defined limit when surface tension and mass are set to zero. Thus we will carry out our calculations in the presence of the tension  $\sigma$  and the mass  $m$ , and set  $\sigma \rightarrow 0$  and  $m \rightarrow 0$  at the end.

The ultraviolet regularization is introduced by a short-distance cutoff  $a$  in the free propagators in coordinate space:

$$\begin{aligned} G_{\phi\phi}^0(x, a) &= \frac{4\pi^2\beta K}{p^2} \int \frac{d^2q}{(2\pi)^2} \frac{e^{iq \cdot y}}{q^2 + m^2} \Big|_{y^2=x^2+a^2} \\ &= \frac{4\pi^2\beta K}{p^2} \frac{1}{2\pi} K_0(m\sqrt{x^2+a^2}) \\ &\sim -\frac{1}{4\pi} \frac{4\pi^2\beta K}{p^2} \ln[cm^2(x^2+a^2)], \\ & \qquad \qquad \qquad m\sqrt{x^2+a^2} \ll 1, \quad (1.10) \end{aligned}$$

and

$$\begin{aligned}
 G_{\nabla h \nabla h}^0(x, a) &= \frac{1}{\beta\kappa} \int \frac{d^2q}{(2\pi)^2} \frac{e^{iq \cdot y}}{q^2 + \sigma} \Big|_{y^2=x^2+a^2} \\
 &= \frac{1}{\beta\kappa} \frac{1}{2\pi} K_0(\sigma^{1/2} \sqrt{x^2 + a^2}) \\
 &\sim -\frac{1}{4\pi} \frac{1}{\beta\kappa} \ln[c\sigma(x^2 + a^2)] , \\
 \sqrt{\sigma(x^2 + a^2)} &\ll 1. \quad (1.11)
 \end{aligned}$$

The Fourier transforms of these functions are

$$\begin{aligned}
 G_{\phi\phi}^0(q, a) &= \frac{4\pi^2\beta K}{p^2} \frac{a\sqrt{q^2 + m^2}}{q^2 + m^2} K_1(a\sqrt{q^2 + m^2}) \\
 &\sim \frac{4\pi^2\beta K}{p^2} \frac{1}{q^2 + m^2} , \quad a \rightarrow 0, \quad (1.12)
 \end{aligned}$$

and

$$\begin{aligned}
 G_{\nabla h \nabla h}^0(q, a) &= \frac{1}{\beta\kappa} \frac{a\sqrt{q^2 + \sigma}}{q^2 + \sigma} K_1(a\sqrt{q^2 + \sigma}) \\
 &\sim \frac{1}{\beta\kappa} \frac{1}{q^2 + \sigma} , \quad a \rightarrow 0, \quad (1.13)
 \end{aligned}$$

where  $K_0(x)$  and  $K_1(x)$  are the conventional Bessel functions [4] and  $c = e^{2\gamma}/4$  with  $\gamma$  the Euler constant. We use this ultraviolet regularization rather than the sharp cutoff in momentum space since our calculations can be easily evaluated in coordinate space [3,5,6].

### II. RG RECURSION RELATIONS

In order to establish the RG recursion relations for the bending rigidity, the hexatic rigidity, and the fugacity of the fluctuating hexatic membranes, we study the renormalizations of the two-point vertex functions  $\Gamma_{\phi\phi}^{(2)}(q)$  and  $\Gamma_{hh}^{(2)}(q)$  for the total Hamiltonian in (1.1). We have two independent sets of expansion parameters that are small. One consists of the single parameter  $(\beta\kappa)^{-1}$ ; the other consists of the expansion parameters of the two-dimensional XY model: the deviation of the hexatic rigidity from the fixed point value,  $\delta = (\pi\beta K/2p^2) - 1$ , and the fugacity of the disclinations,  $y$ . We will carry out calculations to lowest order in temperature  $[(\beta\kappa)^{-1}]$  and combined second order in  $\delta$  and  $y$ . Thus we divide the renormalization scheme into two separate parts; first we obtain the vertex functions  $\tilde{\Gamma}^{(2)}$  for  $y = 0$  up to first order in temperature, then we turn on the effect of the disclinations ( $y \neq 0$ ) and calculate the vertex functions  $\Gamma^{(2)}$  up to combined second order in  $\delta$  and  $y$ .

Starting with  $y = 0$ , we calculate the two-point vertex function  $\tilde{\Gamma}_{\phi\phi}^{(2)}$  for the sine-Gordon field  $\phi$  to lowest order in temperature. The only diagram contributing to  $\tilde{\Gamma}_{\phi\phi}^{(2)}$  in this limit is shown in Fig. 1. It arises from the coupling of  $\phi$  to  $h$ . When  $\sigma = 0$ , the resulting vertex can be written as

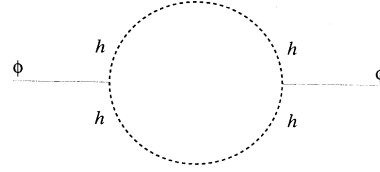


FIG. 1. Diagram contributing to the shift of the stiffness.

$$\tilde{\Gamma}_{\phi\phi}^{(2)}(q) = \left( \frac{p^2}{4\pi^2\beta K} + \frac{p^2}{4\pi^2} \frac{3}{32\pi} \frac{1}{(\beta\kappa)^2} \right) q^2 + \frac{p^2}{4\pi\beta K} m^2. \quad (2.1)$$

Thus, the effect of height fluctuation is to shift the hexatic rigidity from  $K$  to  $\bar{K}$ , where to leading order in temperature  $[(\beta\kappa)^{-1}]$

$$(\beta\bar{K})^{-1} = (\beta K)^{-1} + \frac{3}{32\pi} (\beta\kappa)^{-2}. \quad (2.2)$$

Now taking into account the effect of the disclinations, we calculate  $\Gamma_{\phi\phi}^{(2)}$  up to second order in  $\delta$  and  $y$ . The first step in the computation of  $\Gamma_{\phi\phi}^{(2)}$  is the summation of tadpoles. By expanding the  $\cos\phi$  interaction of the sine-Gordon Hamiltonian in powers of  $\phi$ , one generates diagrams composed of vertices of all even orders and bare propagator  $G_{\phi\phi}^0(q, a)$ . In Ref. [7], Coleman noted that only diagrams containing tadpoles are ultraviolet-divergent logarithmically and these divergences can be removed by renormalizing the fugacity  $y$ . Tadpole diagrams are shown in Fig. 2. The effect of tadpoles is to renormalize  $y$ . Any diagram can be described as a diagram without tadpoles plus tadpoles adjoined. The effect of adding an arbitrary number of tadpoles to a bare vertex is to multiply each vertex by

$$e^{-\frac{1}{2}G_{\phi\phi}^0(x=0,a)}, \quad (2.3)$$

thereby renormalizing  $y$ :

$$\begin{aligned}
 ya^{-2} &\rightarrow ya^{-2} e^{-\frac{1}{2}G_0(x=0,a)} \\
 &= ycm^2(cm^2a^2)^{\frac{\pi\beta K}{2n^2}A-1} \equiv y\mathcal{A}, \quad (2.4)
 \end{aligned}$$

where the last equation defines  $\mathcal{A}$ .

Next we introduce some diagrammatic notation. The sum of even numbers of intermediate propagators is  $[\cosh G_{\phi\phi}^0(x) - 1]$ , and the sum of odd numbers of intermediate propagators is  $[\sinh G_{\phi\phi}^0(x) - G_{\phi\phi}^0(x)]$ . The diagrams corresponding to these sums are shown in Figs.

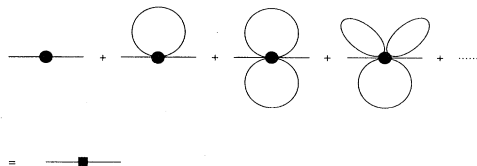


FIG. 2. Circular dot represents the  $\cos$  interaction and the square dot represents the sum of tadpole diagrams.

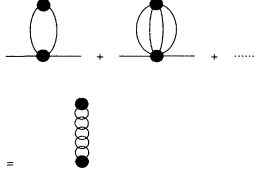


FIG. 3. Sum of even numbers of intermediate propagators is represented by the vertical line of circles.

3 and 4. Using this notation, all diagrams contributing to  $\Gamma_{\phi\phi}^{(2)}$  up to second order in  $\delta$  and  $y$  are shown in Fig. 5. Their sum can be written as

$$\begin{aligned} \Gamma_{\phi\phi}^{(2)}(q) &= \frac{p^2}{4\pi^2\beta\bar{K}}(q^2 + m^2) + 2y\mathcal{A} \\ &- (y\mathcal{A})^2 \int d^2x \left\{ e^{iq\cdot x} [\sinh G_{\phi\phi}^0(x) - G_{\phi\phi}^0(x)] \right. \\ &\left. - [\cosh G_{\phi\phi}^0(x) - 1] \right\}. \end{aligned} \quad (2.5)$$

To second order in  $\delta$  and  $y$ , the first-order term in  $y$  contributes a factor of  $\ln a$ :

$$y\mathcal{A} = ycm^2(cm^2a^2)^{\frac{\pi\beta\bar{K}}{2p^2}-1} = ycm^2[1 + \delta \ln(cm^2a^2)], \quad (2.6)$$

where  $\delta = (\pi\beta\bar{K}/2p^2) - 1$ . The divergent part of the second-order term in  $y$  has no  $q^2$ -independent part. When we expand  $e^{iq\cdot x}$  in powers of  $q$ , the odd terms in  $q$  vanish when integrated over angles. To second order in  $\delta$  and  $y$ , the coefficient of  $q^2$  in  $\Gamma_{\phi\phi}^{(2)}$  is

$$\begin{aligned} &\frac{(ycm^2)^2}{4} \int d^2x x^2 [\sinh G_0(x) - G_0(x)] \\ &= \frac{(ycm^2)^2}{4} \int_0^{m^{-1}} \frac{\pi x^3 dx}{[cm^2(x^2 + a^2)]^{2+2\delta}} + (\text{finite terms}). \end{aligned} \quad (2.7)$$

$$\begin{aligned} \Gamma_{R\phi\phi}^{(2)} &= \frac{p^2}{4\pi^2\beta\bar{K}_r Z_K^{-1}}(q^2 + m^2) + 2y_r Z_y cm^2 \left[ 1 + \left( \frac{\pi\beta\bar{K}_r Z_K^{-1}}{2p^2} - 1 \right) \ln(cm^2a^2) \right] - \frac{\pi}{32} (2y_r)^2 q^2 \ln(cm^2a^2), \\ &= \frac{p^2}{4\pi^2\beta\bar{K}_r}(q^2 + m^2) + 2y_r cm^2 + \left[ (Z_K - 1) \frac{p^2}{4\pi^2\beta\bar{K}_r} - \frac{\pi}{2} y_r^2 \ln(cm^2a^2) \right] q^2 \\ &+ 2y_r \left[ (Z_y - 1) + \left( \frac{\pi\beta\bar{K}_r Z_K^{-1}}{2p^2} - 1 \right) \ln(cm^2a^2) \right] cm^2. \end{aligned} \quad (2.12)$$

The coefficients  $Z_K$  and  $Z_y$  are chosen so that  $\Gamma_{R\phi\phi}^{(2)}$  is finite in the limit  $a \rightarrow 0$ :

$$Z_K(\mu) = 1 + y_r^2 \frac{2\pi^3\beta\bar{K}_r}{p^2} \ln \mu^2 a^2, \quad (2.13)$$

$$Z_y(\mu) = 1 - \left( \frac{\pi\beta\bar{K}_r}{2p^2} - 1 \right) \ln \mu^2 a^2, \quad (2.14)$$

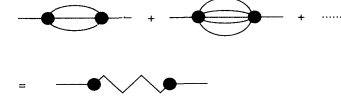


FIG. 4. Sum of odd numbers of intermediate propagators is represented by the sawtooth line.

The integral contributes a factor of  $\ln a$ :

$$2(cm^2)^2 \int_0^{m^{-1}} \frac{x^3 dx}{[cm^2(x^2 + a^2)]^{2+2\delta}} = \int_0^{m^{-1}} \frac{z dz}{(z + a^2)^2} = -\ln(cm^2a^2). \quad (2.8)$$

The leading divergent contribution to  $\Gamma^{(2)}$  is thus

$$\begin{aligned} \Gamma_{\phi\phi}^{(2)}(q) &= \frac{p^2}{4\pi^2\beta\bar{K}}(q^2 + m^2) + 2ycm^2[1 + \delta \ln(cm^2a^2)] \\ &- \frac{\pi}{32} (2y)^2 q^2 \ln(cm^2a^2). \end{aligned} \quad (2.9)$$

To establish the RG recursion relations for the hexatic rigidity  $(\beta\bar{K})^{-1}$  and the fugacity  $y$ , we define renormalized parameters  $(\beta\bar{K}_r)^{-1}$  and  $y_r$  via

$$(\beta\bar{K})^{-1} = Z_K(\beta\bar{K}_r)^{-1}, \quad y = Z_y y_r. \quad (2.10)$$

All infinities can be absorbed by two independent renormalization constants.  $Z_K$  and  $Z_y$  can be chosen as functions of  $a$  to ensure that the renormalized two-point vertex,

$$\Gamma_{R\phi\phi}^{(2)}(q, y_r, \delta_r, \mu) = \Gamma^{(2)}(q, y, \delta, a), \quad (2.11)$$

is finite for some arbitrary length scale  $\mu$ , order by order in a double expansion in  $y_r$  and  $\delta_r = (\pi\beta\bar{K}_r/2p^2) - 1$ , in the limit  $a \rightarrow 0$ . Thus we expand  $Z_K$  and  $Z_y$  in a double series in  $y_r$  and  $\delta_r$ . These expansions are substituted into Eq. (2.10), which in turn are inserted in Eq. (2.9). Then, terms of  $\Gamma_{\phi\phi}^{(2)}$  are rearranged by orders in the double expansion. The coefficient in  $Z_K$  and  $Z_y$  are determined by the requirement that  $q^2$  and  $m^2$  have finite coefficients as follows:

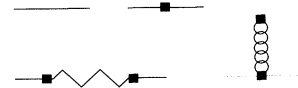


FIG. 5. Diagrams contributing to  $\Gamma_{\phi\phi}^{(2)}$  up to second order in  $y$ . The square dot represents the sum of tadpole diagrams in Fig. 2, the verticle line of circles the sum of even numbers of propagators shown in Fig. 3, and the sawtooth line the sum of odd numbers of propagators shown in Fig. 4.

where  $\mu$  is an arbitrary mass scale. From the renormalization constants derived above, we obtain the RG recursion relations

$$\begin{aligned} \mu \frac{\partial y_r}{\partial \mu} \Big|_b &= -y_r \mu \frac{\partial \ln Z_y}{\partial \mu} \Big|_b \\ &= \left( \frac{\pi \beta \bar{K}_r}{p^2} - 2 \right) y_r, \end{aligned} \tag{2.15}$$

and

$$\begin{aligned} \mu \frac{\partial (\beta \bar{K}_r)^{-1}}{\partial \mu} \Big|_b &= -(\beta \bar{K}_r)^{-1} \mu \frac{\partial \ln Z_K}{\partial \mu} \Big|_b \\ &= -\frac{4\pi^3}{p^2} y_r^2, \end{aligned} \tag{2.16}$$

where the subscript  $b$  means fixed bare parameters. In terms of length scale  $\mu^{-1} = ae^l$ , these equations are expressed as

$$\frac{d}{dl} (\beta \bar{K})^{-1} = \frac{4\pi^3}{p^2} y^2, \tag{2.17}$$

$$\frac{d}{dl} y = \left( 2 - \frac{\pi \beta \bar{K}}{p^2} \right) y. \tag{2.18}$$

To complete the RG recursion relations for our Hamiltonian, we study the renormalization of  $\Gamma_{hh}^{(2)}(q)$ . We introduce a surface tension term [Eq. (1.8)] to regularize infrared divergences. Strictly speaking, we should renormalize  $\sigma$  [8,9] as well as  $\kappa$ . However, we will set the renormalized tension equal to zero in the end. We will, therefore, consider here only the  $q^4$  contributions to  $\Gamma_{hh}^{(2)}$ , which will determine the renormalization of  $\kappa$ . All diagrams contributing to  $\Gamma_{hh}^{(2)}$  up to first order in temperature and second order in  $\delta$  and  $y$  are shown in Fig. 6. Their sum is written as

$$\begin{aligned} \Gamma_{hh}^{(2)}(q) &= \beta \kappa q^4 + \frac{3}{8\pi} q^4 \ln(c\sigma a^2) - \frac{3}{8\pi} \frac{\beta \bar{K}}{4\beta \kappa} q^4 \ln(cm^2 a^2) \\ &\quad - \frac{3}{8\pi} \frac{16\pi^2}{p^2} \frac{(\beta \bar{K})^2}{4\beta \kappa} (2y) q^4 [1 + \delta \ln(cm^2 a^2)] \\ &\quad - \frac{3}{8\pi} \frac{\pi^3}{4p^2} \frac{(\beta \bar{K})^2}{4\beta \kappa} (2y)^2 q^4 [\ln(cm^2 a^2)]^2. \end{aligned} \tag{2.19}$$

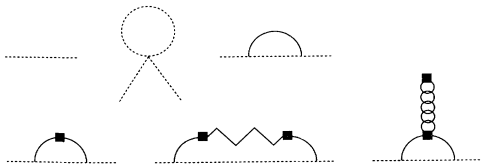


FIG. 6. Diagrams contributing to  $\Gamma_{hh}^{(2)}$  up to one-loop order and second order in  $y$ . The dotted line represents the height fluctuation field  $h$ . The square dot represents the sum of tadpole diagrams in Fig. 2, the verticle line of circles the sum of even numbers of propagators shown in Fig. 3, and the sawtooth line the sum of odd numbers of propagators shown in Fig. 4.

Defining the renormalized parameter  $\kappa_r$  by

$$\kappa = Z_\kappa \kappa_r, \tag{2.20}$$

and using the renormalization constants  $Z_K$  and  $Z_y$  obtained in Eq. (2.13) and Eq. (2.14), we find  $\Gamma_{hh}^{(2)}$  is finite in the limit  $a \rightarrow 0$  if we choose

$$\begin{aligned} Z_\kappa(\mu) &= 1 - \frac{3}{8\pi} \frac{1}{\beta \kappa_r} \ln \mu^2 a^2 + \frac{3}{8\pi} \frac{\beta \bar{K}_r}{4(\beta \kappa_r)^2} \ln \mu^2 a^2 \\ &\quad - \frac{3}{8\pi} \frac{\pi^3}{4p^2} \frac{(\beta \bar{K}_r)^2}{4(\beta \kappa_r)^2} (2y_r)^2 (\ln \mu^2 a^2)^2. \end{aligned} \tag{2.21}$$

The renormalization-group recursion relation for  $\kappa_r$  is

$$\begin{aligned} \mu \frac{\partial \beta \kappa_r}{\partial \mu} \Big|_b &= -\beta \kappa_r \mu \frac{\partial \ln Z_\kappa}{\partial \mu} \Big|_b \\ &= \frac{3}{4\pi} - \frac{3}{4\pi} \frac{\beta \bar{K}_r}{4\beta \kappa_r}, \end{aligned} \tag{2.22}$$

when expressed in terms of  $l = \ln(\mu a)^{-1}$

$$\frac{d}{dl} \beta \kappa = -\frac{3}{4\pi} \left( 1 - \frac{\beta \bar{K}}{4\beta \kappa} \right). \tag{2.23}$$

Thus the complete RG equations for our Hamiltonian are

$$\frac{d}{dl} (\beta \bar{K})^{-1} = \frac{4\pi^3}{p^2} y^2, \tag{2.24}$$

$$\frac{d}{dl} y = \left( 2 - \frac{\pi \beta \bar{K}}{p^2} \right) y, \tag{2.25}$$

$$\frac{d}{dl} \beta \kappa = -\frac{3}{4\pi} \left( 1 - \frac{\beta \bar{K}}{4\beta \kappa} \right). \tag{2.26}$$

These equations and crinkled-to-crumpled phase transition are analyzed in the preceding paper.

### III. ASYMMETRY IN THE DISCLINATION FUGACITIES

On rigid flat membranes, a single positive disclination and a single negative disclination have the same energy proportional to  $\ln(R/a)$ , where  $R$  is the linear dimension of the membrane and  $a$  is the size of the core region of the disclination. However, the plus-minus disclination energy symmetry present in rigid membranes is broken in deformable membranes [10]. For deformable membranes, the topological charges  $q = \pm 1/6$  of the disclinations can partially be canceled by the curvature charges due to the Gaussian curvature, when membranes buckle out to form a cone or a saddle surface. Membranes with a single disclination undergo a mechanical buckling transition from a flat configuration to a cone configuration for a positive disclination or a saddle configuration for a negative disclination. The Coulombic interaction be-

tween disclinations can be screened by Gaussian curvatures, and the disclination energies are reduced in deformable membranes due to buckling into the third dimension. Furthermore, the energy of the cone is lower than that of the saddle, though both energies are proportional to  $\ln(R/a)$  [11]. The system creates and destroys disclinations to minimize its free energy, and, in the hexatic phase, it will always choose configurations in which there is no overall  $\ln(R/a)$  term in the energy. In flat membranes, this term can be eliminated by the condition of charge neutrality. In membranes whose shape can change, this term can also be eliminated by an average flat configuration and the condition of charge neutrality. We believe that this is the most likely scenario, however, it is not impossible that there are curved configurations with an overall unbalanced charge that manage to eliminate the  $\ln(R/a)$  energy. Here we will consider only charge neutral configurations. Local buckling may lead to different fugacities  $y_+$  and  $y_-$  for positive and negative disclinations. However, because of the constraint of charge neutrality, physical observables such as the free energy will depend only on the product  $y_+y_-$ .

We can generalize our charge neutral renormalization calculation to take into account an asymmetry in positive and negative disclination fugacities. Using the Hamiltonian in Ref. [1] with different fugacities for positive and negative disclinations  $y_+$  and  $y_-$ , respectively, we modify the sine-Gordon model as follows:

$$\mathcal{Z} = \int \mathcal{D}\phi \mathcal{D}\mathbf{R} e^{-\beta\mathcal{H}_\kappa - \beta\mathcal{H}_\phi - i(p/2\pi) \int d^2u \sqrt{g} S\phi}, \quad (3.1)$$

where

$$\beta\mathcal{H}_\kappa = \frac{1}{2}\beta\kappa \int d^2u \sqrt{g} H^2, \quad (3.2)$$

and

$$\begin{aligned} \beta\mathcal{H}_\phi = & \frac{1}{2\beta\bar{K}} \left( \frac{p}{2\pi} \right) \int d^2u \sqrt{g} g^{\alpha\beta} \partial_\alpha \phi \partial_\beta \phi \\ & - \frac{(y_+ + y_-)}{a^2} \int d^2u \sqrt{g} \cos \phi - i \frac{(y_+ - y_-)}{a^2} \\ & \times \int d^2u \sqrt{g} \sin \phi. \end{aligned} \quad (3.3)$$

Following the same renormalization scheme as above, we find the recursion relations for the bending rigidity, the

hexatic rigidity, and the fugacities for positive and negative disclinations:

$$\frac{d}{dl} (\beta\bar{K})^{-1} = \frac{4\pi^3}{p^2} y_+ y_-, \quad (3.4)$$

$$\frac{d}{dl} y_\pm = \left( 2 - \frac{\pi\beta\bar{K}}{p^2} \right) y_\pm, \quad (3.5)$$

$$\frac{d}{dl} \beta\kappa = -\frac{3}{4\pi} \left( 1 - \frac{\beta\bar{K}}{4\beta\kappa} \right). \quad (3.6)$$

Defining  $y = \sqrt{y_+ y_-}$  and  $z = \sqrt{y_+ / y_-}$ , we find

$$\frac{d}{dl} (\beta\bar{K})^{-1} = \frac{4\pi^3}{p^2} y^2, \quad (3.7)$$

$$\frac{d}{dl} y = \left( 2 - \frac{\pi\beta\bar{K}}{p^2} \right) y, \quad (3.8)$$

$$\frac{d}{dl} z = 0. \quad (3.9)$$

Equations for  $y$  and  $\bar{K}$  are identical to the symmetric case. The equation for  $z$  implies the ratio  $y_+ / y_-$  does not change under RG. Thus in the ordered phase,  $y_+$  and  $y_-$  scale to zero and the KT transition occurs at the same temperature as in symmetric case.

For  $T > T_{KT}$ , both  $y_+$  and  $y_-$  grow. If there is an initial asymmetry between  $y_+$  and  $y_-$ , it will persist, and positive disclinations will be favored over negative ones. This presumably favors positive Gaussian curvature. A complete discussion of the fluid phase would then require a more complete treatment of Gaussian curvature. The flat phase and the Kosterlitz-Thouless transition are, as we have just seen, not affected by an asymmetry in positive and negative disclination fugacities.

This work was supported in part by NSF Grant No. DMR 91-22645 and by the Penn Laboratory for research in the Structure of Matter under NSF Grant No. 91-20668.

- 
- [1] J.M. Park and T.C. Lubensky, preceding paper, Phys. Rev. E **53**, 2648 (1996).  
 [2] D.J. Amit, *Field Theory, the Renormalization Group, and Critical Phenomena* (World Scientific, Singapore, 1984).  
 [3] D.J. Amit, Y.Y. Goldschmidt, and G. Grinstein, J. Phys. A **13**, 585 (1980).  
 [4] H. Bateman, *Higher Transcendental Functions* (McGraw-Hill, New York, 1953), Vol. 2.  
 [5] J. Zinn-Justin, *Quantum Field Theory and Critical Phenomena* (Clarendon Press, Oxford, 1989).  
 [6] C. Itzykson and J. Drouffe, *Statistical Field Theory*

- (Cambridge University Press, Cambridge, 1989).  
 [7] S. Coleman, Phys. Rev. D **11**, 2088 (1975).  
 [8] F. David, E. Guitter, and L. Peliti, J. Phys. (Paris) **48**, 2059 (1987).  
 [9] W. Cai, T. Lubensky, T. Powers, and P. Nelson, J. Phys. II (France) **4**, 931 (1994).  
 [10] D.R. Nelson, in *Defects in Superfluids, Superconductors, and Membranes*, 1994 Les Houches Lectures, Session LXII, edited by F. David, P. Ginsparg, and J. Zinn-Justin (Elsevier, Amsterdam, 1995).  
 [11] J.M. Park and T.C. Lubensky J. Phys. (France) I (to be published).